Optimal Allocation of Land Area for a Hybrid Solar Wind Power Plant

Neha Sengupta, Kaushik Das, T.S. Jayram, Deva P. Seetharam
IBM Research, India
neha.sengupta@in.ibm.com, kausdas8@in.ibm.com, t.s.jayram@in.ibm.com, dseetharam@in.ibm.com,

***Abstract*—Recently, there has been a growing interest in wind solar hybrid power plants as a means to overcome the inherent intermittency in both resources. One crucial decision faced by a hybrid plant designer is to determine an allocation of land area between wind and solar installations so as to satisfy the generation requirements in terms of the power output by the plant along with the availability. In this paper, a methodology is proposed for this optimal allocation problem under the constraints of climate and weather conditions, land area available for renewable energy harvesting, and PV/ wind turbine characteristics. Based on historical wind speed and solar insolation data for a given location, probabilistic models using parametric and non parametric estimation techniques are developed to capture the variability and periodicity in these resources. A probabilistic model for the hybrid system is also derived using which the optimal allocation that satisfies the generation requirements is determined. The proposed method is validated by performing a detailed experimental analysis on historical data for an arbitrary location on the globe.**

I. Introduction

Renewable energy resources, such as wind and solar, are considered highly promising in the face of growing concerns for the environment, energy conservation, and sustainable development [1]. Daily as well as seasonal variability are inherent to both wind and solar resources [2]. Traditionally, the uncertainty of a standalone solar panel or wind turbine installation is managed using a storage system. However, this results in an increased overall cost of the output energy, and therefore limits the benefits of using renewable energy [3]. A hybrid solar wind energy system uses two renewable energy sources, thereby improving the system efficiency and power reliability, and reducing the energy storage requirement [4]. However, aggregating inherently stochastic power sources such as wind and solar to achieve reliable electricity supply is a non trivial problem [5].

Consider the scenario of a typical market model described in [6], wherein each day at a specified hour, the owner of the plant establishes a schedule of the net power export to the grid for each hour of the next day. Power is traded in a day-ahead spot market, and any deviations from the contracted power due to forecast errors are settled in a balancing market. For the hybrid plant owner who bids in this market, this has serious implications in terms of managing the risk induced by the uncertain renewable energy sources. It follows that the question of characterizing the reliability of a given hybrid installation must be answered for meaningful market participation. This is also relevant to the planning phase of a hybrid plant, in which the sizing of wind and solar installations must be optimized in order to maximize magnitude and availability of energy output.

The availability of wind and solar energy at a given location depends on climate and weather conditions and is highly variable [4]. Therefore, a prediction model for these resources should be stochastic in nature to be able to account for the inherent variability. A majority of the existing tools for forecasting these renewable resources give a deterministic forecast, also known as a spot or a point forecast. This is a single value for each forecast horizon. Such methods suffer from the drawback that they provide no information about any departure from the prediction. In decision-making applications based on stochastic optimization or risk assessment, a point forecast finds limited use. It has been shown that for trading future production on an electricity market as described above, using probabilistic predictions rather than point forecasts yeilds greater benefits [3]. In [7] First Order and Second Order Markov Chain Models are used to develop a purely statistical and probabilistic wind power forecasting method. Both models are applied on a wind power dataset and their performances are compared with that of a Persistent Model. [3] uses non-parametric estimation techniques to build probability density functions for wind speed forecasting. AI techniques like artificial neural networks, fuzzy logic, genetic algorithms, and wavelet neural networks have been used for solar power prediction. [8] gives an overview of all these methods as applied to the problem of PV sizing.

Various optimization techniques for hybrid PV/wind systems sizing have been proposed in the literature. Wang et. al. [5] discussed the applicability of the concepts of stochastic network calculus to analyze the achievable level of system reliability with appropriate number of PV cells, wind turbines, and energy storage capacity. One source of difficulty in applying stochastic network calculus is obtaining reliable supply and demand models. Tina et al. [2] presented a probabilistic approach based on the convolution technique to assess the long-term performance of a hybrid solar-wind power system (HSWPS) for both stand-alone and grid-linked applications. They generated the probability distribution functions (pdf) for wind and solar power using parametric estimation methods. The size of PV and wind are chosen such that the energy that cannot be supplied to fulfill the demand is minimized. An optimization problem is formulated to choose the most cost-effective combination. Terra et. al. [9] proposed a procedure to obtain the optimal sizing of a grid connected HSWPS that involves fuzzy logic based multi-objective optimization. The optimization technique depends on how well the hybrid system can satisfy the demand. Borowy et. al. [10] presented a method for calculating the optimum size of a battery bank and the PV array of a standalone hybrid Wind-PV system that satisfies the demand profile of a given location. Yang et. al. [11] proposed a method to calculate the optimum system configuration that can achieve the customers required loss of power supply probability with a minimum annualized cost of system based on a genetic algorithm. Yang et. al. [12] developed a sizing model that optimizes the capacity sizes of different components of HSPWS employing a battery bank using an iterative technique. All the above methods rely on load profile to obtain their solutions. But access to load data is one of the most important and difficult steps in planning and operation of distribution systems [13].

Our contributions include:

- A comprehensive performance assessment technique for a wind-solar hybrid system based on local climate and weather conditions, land area available for renewable energy harvesting, and device limitations.
- Performance evaluation based on measures of energy throughput and availability, so as to assist the risk/energy trade-off decision faced by the system planner.
- Use of the above analysis to optimally size the wind and solar installations in a given land area for a given requirement of availability.

II. Problem Formulation

Optimal Mix Problem: We consider a problem where a hybrid power plant needs to be set up in a given land area at a particular latitude/ longitude on the globe. Given the total area of land available for renewable energy harvesting, an optimal mix determines the best way to divide the land into the wind and the solar resource installations based on year round availability and maximum power output. A hybrid plant is said to output power P with an availability of L, if at least P MW of power is generated $L\%$ of the time over the year. The factors to be considered are the historical behavior of the weather of that location (obtained by extracting data for the particular latitude/ longitude from a global weather dataset), wind turbine and solar panel specific parameters.

III. Algorithm

The input to the algorithm consists of the following.

- Total land area
- Latitude, Longitude
- Solar panel parameters : Efficiency, rated power, horizontal surface area.
- Wind turbine parameters : Rotor diameter, land area required, turbine efficiency, rated power, cut-in, cut-off, and rated wind speeds.
- Required Availability

The algorithm outputs the optimal mix in terms of

- Fraction of land to devote to wind turbine installation
- Fraction of land to devote to solar panel installation

An overview of the steps in the algorithm can be written as:

1) Extract weather data for wind speed and solar insolation
2) Identify patterns in the data and the best way to slice it into multiple time horizons
3) Generate wind speed and solar insolation pdfs for each time horizon individually
4) Identify and enumerate feasible wind-solar mixes in the land area
5) Build the *mix table* for a given availability L as follows, for each feasible mix m, and for every time horizon k
   a) Transform the result of (3) to solar and wind power pdfs.
   b) Convolve the above to get a pdf for the hybrid power P_{Hybrid}.
   c) Set $mixTable[m,k] = \beta$, such that $Prob(P_{Hybrid} \geq \beta) = L$
6) Normalize the mix table for each of the columns, by dividing each element by the maximum value in that column.
7) Take the sum of each row.
8) Choose the mix with highest corresponding row sum as the optimal mix for availability L.

The following describes the above steps in detail.

A. Pattern Identification in the Data and Wind/Solar pdfs

Although wind and solar data suffer from high variability, they follow an annual periodicity with slight variations. We therefore choose to model this variability in terms of a set of pdfs for one year. Moreover, within a certain smaller time frame, this variability is typically uniform. As a result, within this time frame, a single pdf can represent the variation. We slice the data in different ways in order to determine which slicing captures the nature of the data best. The data can be sliced monthly, weekly, hourly, or a combination of these ways.

We consider the following 4 ways to slice the data -

- **Month (M)**: Resulting in 12 pdfs, one for each month
- **Week (W)**: Resulting in 52 pdfs, one for each week
- **Month and 3 hours (MH3)** : Every month is represented by 8 different pdfs, for the 3 hour intervals within a day, to get a total of 96 pdfs for the entire year.
- **Month and 6 hours (MH6)** : Like the above, except the variability is thought to change every 6 hours. Results in a total of 48 pdfs for the year.

For each of the ways listed above, we estimate pdfs for wind speed and solar insolation for all the slices.

1) Pdf Generation: The objective is to determine pdfs $f(x_s)$, and $f(x_w)$ for the continous variables x_s (solar insolation) and x_w (wind speed). The pdfs are generated using parametric and non parametric methods. In the parametric framework, a family of distributions is chosen e.g. a Gaussian distribution. Then, the parameters of the distribution are estimated from the data. In the non-parametric framework the distribution is directly estimated from the data with weaker hypothesis on the underlying distribution. The main drawback of the non-parametric approach is that it requires larger data sets than the parametric approach to attain equivalent estimations, whereas the advantage is that it limits estimation errors due to incorrect hypothesis on the underlying distribution family[3].

a) Non-Parametric: In statistics, kernel density estimation (KDE) is a non-parametric way to estimate the probability density function of a random variable. Kernel density estimates are closely related to histograms, but can be endowed with properties such as smoothness or continuity by using a suitable kernel. The general form of kernel density estimate for a random variable x from a population $\{x_1, x_2, ..., x_n\}$ is given by

$$\hat{f}(x) = \frac{1}{nh}\sum_{i=1}^{n} K\left(\frac{x - x_i}{h}\right) \tag{1}$$

where h is the bandwidth which controls the degree of smoothing in the estimate. Kernel Density Estimation can employ various different kernels depending on the data. For our purpose, we have selected the Epanechnikov kernel given by [14],

$$K(t) \begin{array}{l} = \frac{3}{4}\left(1 - \frac{1}{5}t^2\right)/\sqrt(5), \quad \text{for}|t| < \sqrt(5) \\ = 0, \quad \text{otherwise} \end{array} \tag{2}$$

b) Parametric: In order to account for the variability of wind speed, it is assumed to be characterized by a Weibull distribution with a scale parameter λ and a shape parameter k. Density and distribution probability functions are given by

$$f_v = \frac{k}{\lambda^k} v^{(k-1)} exp[-(\frac{v}{\lambda})^k] \tag{3}$$

$$F_v = 1 - exp[-(\frac{v}{\lambda})^k] \tag{4}$$

For the selected time slice, the parameters λ and k are calculated using Maximum Likelihood Estimation(MLE). closed-form characterization of ML parameter estimates $\hat{k}$ and $\hat{\lambda}$ are:

$$\hat{\lambda} = \left[\frac{1}{n}\sum_{i=1}^{n} v_i^{\hat{k}}\right]^{1/\hat{k}} \tag{5}$$

$$\frac{1}{\hat{k}} + \frac{1}{n}\sum_{i=1}^{n} ln v_i - \sum_{i=1}^{n} v_i^{\hat{k}} ln v_i / \sum_{i=1}^{n} v_i^{\hat{k}} = 0 \tag{6}$$

where, v denotes the population of wind speed given by $\{v_1, v_2, ..., v_i, ..., v_n\}$ [15].

For solar, the modified gamma distribution is used. This distribution models k_t, where k_t is the clearness index given by the ratio of the average horizontal insolation at the site I_H to the extraterrestrial insolation on a horizontal surface above the site and just outside the atmosphere, I_0. k_t is suitable to be modeled by a parametric distribution function because it has been seen that if two sets of data have same mean value of k_t, they will generate similar $f(k_t)$ functions [16], The modified gamma distribution function for k_t is given by:

$$f_{k_t} = C\frac{(k_{tu} - k_t)}{k_{tu}} exp(\lambda_s k_t) \tag{7}$$

where, $k_{tl} \leq k_t \leq k_{tu}$. C and λ_s are functions of k_{tu} and $\bar{k_t}$ given by

$$C = \lambda_s^2 k_{tu}/(exp(\lambda_s k_{tu}) - 1 - \lambda_s k_{tu}) \tag{8}$$

$$\lambda_s = (2\Gamma - 17.519 exp(-1.3118\Gamma) - 1062 exp(-5.0426\Gamma))/k_{tu} \tag{9}$$

where, $\Gamma = k_{tu}/(k_{tu} - \bar{k_t})$

2) Selection of best slice: Pdfs generated using parametric and non-parametric methods are evaluated to select the most relevant slice. The pdfs are evaluated for the estimation accuracy using a modified estimator for the well known measure of Mean Integrated Square Error.

$$MCV(\hat{f}) = \int \hat{f}(x)^2 dx - \frac{2}{n}\sum_{i=1}^{n} \hat{f}_{-i}(x_i) \tag{10}$$

where $\hat{f}_{-i}(x)$ is the estimated density at argument x using the original sample apart from observation x_i [14].
The slicing for which minimum mcv values are obtained, is selected as the best slicing.

B. Identification of Feasible Mixes

The various possible mixes that the land area can accommodate is identified in this step. The wake effect seen in wind systems mandate that wind turbines be placed at least 5 to 10 rotor diameters apart from each other. Let us say that $A_{footprint}$ is the area occupied by one wind turbine, and A_{wake} is the total area that each wind turbine needs around itself for the system as a whole to overcome the wake effect. Let A_{total} be the total land area available. Then the maximum number of wind turbines that can be installed in this land area is $tm = A_{total}/A_{wake}$. Let $0 \leq k \leq tm$ be the number of wind turbines installed in a given mix. Then the wind installation occupies an area of $A_w = k.A_{footprint}$, and so the solar panels can be installed over an area of $A_s = A_{total} - A_w$.

C. Pdf Transformation

With the selected slice and for each identified mix, the generated pdfs for wind speed and solar insolation / clearness index are converted to pdfs for wind power and solar power

1) wind speed to wind power: $P_w(v)$ is defined as

$$P_w(v) = \begin{cases} \alpha v^3 & \text{, for } V_C \leq v \leq V_R \\ P_R & \text{, for } V_R \leq v \leq V_F \\ 0 & \text{, otherwise} \end{cases} \tag{11}$$

where $\alpha = \frac{1}{2}\eta_w \rho A_w$
Using the above, the wind power pdf is calculated as,

$$f_{P_w}(P_w) = \begin{cases} F_1 & P_w = 0 \\ f_v((\frac{P_w}{\alpha})^{1/3}).\frac{1}{3}\left(\frac{\alpha}{P_w}\right)^{2/3} & 0 < P_w < P_R \\ F_2 & P = P_R \end{cases} \tag{12}$$

where,

$$F_1 = 1 - [F_v(V_F) - F_v(V_C)] \tag{13}$$

$$F_2 = F_v(V_F) - F_v(V_R) \tag{14}$$

V_C is cut in speed, V_R is rated speed, and V_F is cut out speed of wind for the wind turbine.

2) Insolation/ clearness Index to solar Power: For insolation,

$$P_{pv} = \eta_s A_s I_h \tag{15}$$

$$f_{P_{pv}}(P_{pv}) = f_{I_h}\left(\frac{P_{pv}}{\eta_s A_s}\right)\frac{1}{\eta_s A_s} \tag{16}$$

For clearness index,

$$P_{pv} = \eta_s A_s k_t I_{ET} \tag{17}$$

$$f_{P_{pv}}(P_{pv}) = f_{k_t}\left(\frac{P_{pv}}{\eta_s A_s I_{ET}}\right)\frac{1}{\eta_s A_s I_{ET}} \tag{18}$$

D. Pdf Convolution

Given $f_{P_w}(P_w)$, the pdf for wind power, and $f_{P_{pv}}(P_{pv})$, the pdf for solar power, we obtain $f(P_h)$, the convolved pdf for the hybrid system using the following,

$$f(P_h) = \int_0^U f_{pv}(P_h - P_w).f_{P_w}(P_w)dP_w \tag{19}$$

The upper bound of the above integration depends on the value of P_h.

- If $P_h \leq P_{WR}$, then $U = P_h$
- If $P_h > P_{WR}$, then $U = P_{WR}$

The above convolution can be done numerically as well as analytically.

E. Optimal Mix

For a certain mix of wind and solar, say wind $= a$ and solar $= b$, we build p pdfs, one for each of the p time horizons identified. In order to evaluate the optimal mix, the concept of 'Availability' is considered. The hybrid plant with the power output pdf, P_{ij}, for the i^{th} mix and the j^{th} time horizon, produces power β_{ij} with availability L, if

$$P_{ij}(X \geq \beta_{ij}) = L \tag{20}$$

where,$1 \leq i \leq tm$ and $1 \leq j \leq p$
We build a mix table having a row for each feasible mix, and a column for each time horizon. For the mix i, in time horizon j, $mixTable[i,j] = \beta_{ij}$. Table I shows the structure of the mix table.

TABLE I
MIX TABLE FOR AVAILABILITY = L

Mix	$TimeHorizon_1$	..	$TimeHorizon_p$
mix_1	β_{11}	..	β_{1p}
mix_2	β_{21}	..	β_{2p}
..	..	..	..
mix_{tm}	β_{tm1}	..	β_{tmp}

From Table I, it is easy to infer which mix performs best for a specific time horizon by looking at the corresponding column. Also, one can evaluate the performance of a mix across various time horizons using the corresponding row. It is possible that a certain mix performs very well in a given time horizon and very badly in some other. We must select a mix that is consistent in its performance across the year, while giving a high power throughput. To incorporate the above, the following steps are performed on the mix table to find the optimal mix:

1) Each column is normalized by dividing the values by the maximum in that column.
2) For each row, the sum is taken over all the columns.

The mix that corresponds to the highest row sum is chosen as the best mix for the required reliability L.

IV. Experiments

The experiments were conducted for a land area of 20 acres at the location (33.5, 77.5). Global reanalysis data for wind speed and solar insolation were extracted for this location for the years (2001-2010) over the months (January, April, July, and October). This set of equidistant months was chosen in order to capture the seasonal variation in both resources, while at the same time limiting the large volume of data that is input to the system. The global reanalysis data set used here is the Global Land Data Assimilation System (GLDAS) dataset. GLDAS data are produced by specific instances of the Land Information System (LIS) software framework for high-performance land surface modeling and data assimilation developed within the Hydrological Sciences Branch at NASA Goddard [**?**].

A. Pdf Estimation

1) Wind: Pdfs for wind speed v are generated using non-parametric method and parametric method (Weibull distribution) for all possible ways of data slicing. For the non parametric method, the bandwidth parameter is chosen based on the MCV measure described in section III-A2. On iterating over a range of values for bandwidth, and measuring the MCV for each, the optimal bandwidth (the one for which a minimum MCV was obtained) is arrived at as shown in Figure 1. Pdfs developed using non-parametric methods for the month of January are shown in Figure 2. The MCV measure is also useful in choosing the best way to slice the data. For each of the different slicing ways, MCV was calculated and tabulated as in Table II (shows average MCV values over all slices). Since a smaller MCV is an indicator of higher predictability within the same family of distributions, MH3 was chosen as the best method to slice the data, and as a result 32 pdfs (8 for each month) were obtained over the year for each parameter.

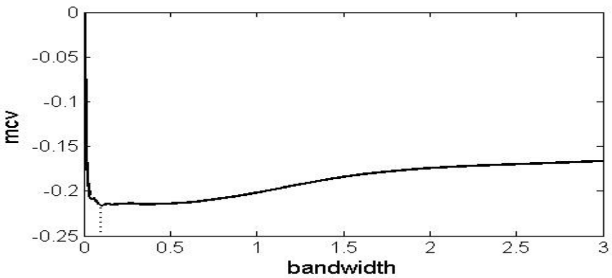

Fig. 1. MCV vs Bandwidth

TABLE II
MCV VALUES FOR WIND SPEED PDFS

SLICES	$MCV_{non-parametric}$	$MCV_{parametric}$
M	-0.17321	-0.269932
MH3	-0.23685	-0.422410
MH6	-0.18822	-0.312177
W	-0.18125	-0.316778

2) Solar: Pdfs for I_h are generated using non-parametric method, and pdfs for k_t are generated using parametric method (Modified Gamma Distribution) for all possible ways of data slicing. Pdfs for M and MH3 developed using non-parametric methods for the month of January are shown in Figure 3. It is helpful in visualizing the effect of slicing on the resultant pdfs. While the pdf based on the whole months data is multimodal, the individual pdfs based on the same data, but sliced by hour, show well defined peaks around specific values.

B. Mix Identification and Pdf Transformation

In identifying the various feasible mixes and obtaining the hybrid power pdfs corresponding to each, device specific parameters for the wind turbine and the solar panel must be incorporated. For our experiments, the following typical values of certain parameters are taken into consideration:

- Wind Turbine Parameters- Cut-in Speed = 3 m/s, Cut-off Speed = 25 m/s, Rated Speed = 13 m/s, $A_{footprint}$ = 0.25 acres, Efficiency = 42%, A_{wake} = 2.5 acres .
- Solar Panel Parameters- Efficiency = 12%

According to these parameter settings, there are 8 feasible mixes : 1^{st} mix has 1 turbine, 2^{nd} mix has 2 turbines and so on. The remaining area of land is dedicated for solar panels.

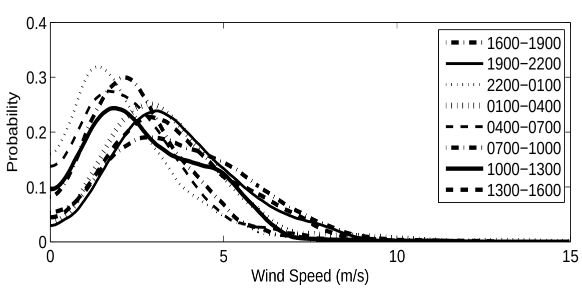

Fig. 2. Wind pdf for MH3 in Jan generated using non-parametric method

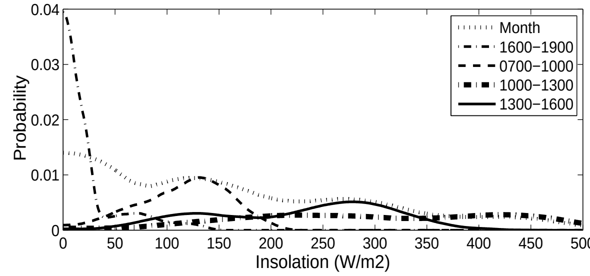

Fig. 3. Solar pdf for Jan generated using non-parametric method

For each mix, the wind speed and solar insolation pdfs for the 32 slices were transformed into wind power and solar power pdfs respectively. These were then convolved using equation 19 to obtain a hybrid power pdf f_{P_h} for each slice. Figure 4 shows the seasonal variation in the power generation of the hybrid installation during the 3 hour interval 1300-1600 hours, for the months of January and July.

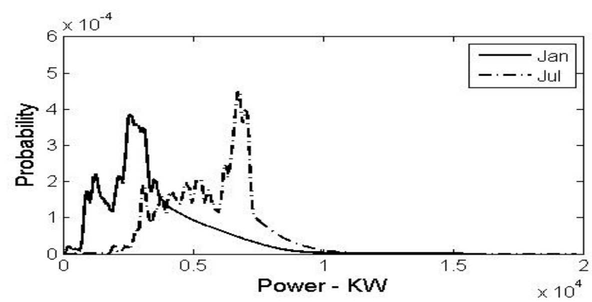

Fig. 4. Hybrid Power pdf for mix 3, hour 1300-1600

C. Optimal Mix

For a given value of availability L, power output values β_{ij} are calculated for all the 9 mixes over the 32 time horizons as given by equation 20. Tables III and IV show the populated mix tables for an availability of 70% for the months of January and July respectively.

TABLE III
POWER OUTPUT FOR AVAILABILITY = 70 % FOR JANUARY (IN MW)

Mix	1-4	4-7	7-10	10-13	13-16	16-19	19-22	22-1
1	0	0	1.16	2.33	2.01	.10	0	0
2	0	0	1.24	2.45	2.20	.10	0	0
3	0	0	1.27	2.51	2.31	.10	0	0
4	0	0	1.28	2.53	2.35	.10	0	0
5	0	0	1.28	2.52	2.36	.10	0	0
6	0	0	1.28	2.51	2.36	.09	0	0
7	0	0	1.27	2.49	2.35	.09	0	0
8	0	0	1.26	2.47	2.34	.09	0	0

In the above tables, there are several time horizons for which power output is zero. These correspond to the night time, when there is no solar energy. During these periods, wind speed fails to exceed the cut in wind speed for the turbines 70% of the time, and hence the power throughput for 70% availability comes out to be zero. It can be observed from Table III that

TABLE IV
POWER OUTPUT FOR AVAILABILITY = 70 % FOR JULY (IN MW)

Mix	1-4	4-7	7-10	10-13	13-16	16-19	19-22	22-1
1	0	.51	3.88	5.24	4.54	1.59	.01	0
2	0	.47	3.79	5.24	4.58	1.60	.01	0
3	0	.59	3.91	5.26	4.60	1.59	.01	0
4	0	.49	3.80	5.25	4.60	1.58	.01	0
5	0	.53	3.88	5.24	4.56	1.57	.01	0
6	0	.49	3.89	5.21	4.57	1.56	.01	0
7	0	.48	3.56	5.17	4.62	1.54	.01	0
8	0	.48	4.13	5.18	4.58	1.52	.01	0

mix 5 performs best for the month of January in terms of total power generation whereas, Table IV depicts that mix 3 performs better than others for the month of July.
In order to determine the most suitable mix which performs best across the year, we performed normalization on the mix table.

The normalized table for the month of January is shown in Table V. The best mix is the one corresponding to the highest row sum in the normalized mix table. The row sums were taken over all the normalized 32 columns. For an availability of 70%, mix 5 is found to be the best.

TABLE V
NORMALIZED MIX TABLE FOR AVAILABILITY = 70 % FOR JANUARY

Mix	1-4	4-7	7-10	10-13	13-16	16-19	19-22	22-1
1	0	0	0.91	0.92	0.85	1	0	0
2	0	0	0.97	0.97	0.93	1	0	0
3	0	0	0.99	0.99	0.98	1	0	0
4	0	0	1	1	0.99	1	0	0
5	0	0	1	0.99	1	1	0	0
6	0	0	0.99	0.98	0.99	0.9	0	0
7	0	0	0.99	0.98	0.99	0.9	0	0
8	0	0	0.98	0.98	0.99	0.9	0	0

Similarly, the optimal mix is determined for different values of availability and shown in Table VI. It is interesting to note the trade-off between availability and minimum energy generated in the considered 4 months. If the availability is high, the minimum energy output is less and vice versa. It can also be noted from Table VI that if the required availability is too low the choice of mix becomes obvious. It reduces to either complete solar or wind installation, depending on which has more potential in the specific location.

TABLE VI
OPTIMAL MIXES FOR VARIOUS AVAILABILITY VALUES

Availability	Best Mix	$Energy_{min}$ in MWh
80 %	5	365583
70 %	5	435612
60 %	7	499689
50 %	8	576879
40 %	8	732468

V. CONCLUSION

In this paper, we have described a probabilistic approach to optimizing the land allocation for a HSWPS. We show that the choice of slicing as applied on data affects the predictive ability of the probabilistic models. Our results validate the intuitively obvious fact that for low availability, the optimal solution tends to allocate an overwhelming fraction of the land resource to one extreme of wind/solarand while for high availability a mix (which is precisely estimated by our methods) of both renewables is desired. While we considered the metric of maximizing power throughput for a given availability, the probabilistic description of the hybrid system is flexible enough to encompass other metrics, e.g. LPSP or EINS, when demand profile is available. Future work includes incorporating cost of devices and the possibility of using multiple types of turbines and solar panels.

REFERENCES

[1] S. Zhang and M. Huang, "Microgrid: A strategy to develop distributed renewable energy resource," in *Electrical and Control Engineering (ICECE), 2011 International Conference on*, sept. 2011, pp. 3520 –3523.

[2] G. Tina, S. Gagliano, and S. Raiti, "Hybrid solar/wind power system probabilistic modeling for long-term performance assessment," *Solar Energy*, vol. 80, no. 5, pp. 578–588, 2006.

[3] J. Juban, N. Siebert, and G. N. Kariniotakis, "Probabilistic short-term wind power forecasting for the optimal management of wind generation," in *Power Tech, 2007 IEEE Lausanne*, 2007, pp. 683–688.

[4] W. Zhou, C. Lou, Z. Li, L. Lu, and H. Yang, "Current status of research on optimum sizing of stand-alone hybrid solarewind power generation systems," *Applied Energy*, vol. 87, no. 2, pp. 380–389, 2010.

[5] K. Wang, S. Low, and C. Lin, "How stochastic network calculus concepts help green the power grid," in *IEEE International Conference on Smart Grid Communications (SmartGridComm)*, 2011, pp. 55–60.

[6] M. Korpas and A. Holen, "Operation planning of hydrogen storage connected to wind power operating in a power market," *Energy Conversion, IEEE Transactions on*, vol. 21, no. 3, pp. 742 –749, sept. 2006.

[7] A. Carpinone, R. Langella, A. Testa, and M. Giorgio, "Very short-term probabilistic wind power forecasting based on markov chain models," in *Probabilistic Methods Applied to Power Systems (PMAPS), 2010 IEEE 11th International Conference on*, june 2010, pp. 107 –112.

[8] A. Mellit, S. A. Kalogirou, L. Hontoria, and S. Shaari, "Artificial intelligence techniques for photovoltaic applications: A review," *Renewable and Sustainable Energy Reviews*, 2009.

[9] G. L. Terra, G. Salvina, and G. M. Tina, "Optimal sizing procedure for hybrid solar wind power systems by fuzzy logic," in *IEEE Mediterranean Electrotechnical Conference*, 2006, pp. 865–868.

[10] B. S. Borowy and Z. M. Salameh, "Methodology for optimally sizing the combination of a battery bank and pv array in a wind/pv hybrid system," *IEEE Transactions on Energy Conversion*, 1996.

[11] H. X. Yang, W. Zhou, L. Lu, and Z. H. Fang, "Optimal sizing method for standalone hybrid solarewind system with lpsp technology by using genetic algorithm," *Solar Energy*, vol. 82, no. 4, pp. 354–367, 2008.

[12] H. X. Yang, L. Lu, and W. Zhou, "A novel optimization sizing model for hybrid solar-wind power generation system," *Solar Energy*, vol. 81, no. 1, 2007.

[13] A. Hadian, M.-R. Haghifam, J. Zohrevand, and E. Akhavan-Rezai, "Probabilistic approach for renewable dg placement in distribution systems with uncertain and time varying loads," in *Power Energy Society General Meeting, 2009. PES '09. IEEE*, july 2009, pp. 1 –8.

[14] W. Zucchini, "Applied smoothing techniques, part 1: Kernel density estimation," 2003, http://isc.temple.edu/economics/Econ616/Kernel/ast_part1.pdf.

[15] A. Tuzuner and Y. Zuwei, "A theoretical analysis on parameter estimation for the weibull wind speed distribution," in *IEEE Power and Energy Society General Meeting - Conversion and Delivery of Electrical Energy in the 21st Century*, 2008, pp. 1–6.

[16] K. G. T. Hollands and R. G. Huget, "A probability density function for the clearnessindex, with applications," *Solar Energy*, vol. 30, no. 3, 1983.